DAMAGE CHARACTERISTICS AND MICROMECHANICS OF IMPACT RESISTANT ENGINEERED CEMENTITIOUS COMPOSITES

E-H Yang[1)] and V. C. Li[2)]
[1)] Exponent, Inc., 10850 Richmond Ave, Suite 175 Houston, TX 77042
[2)] Civil and Environmental Engineering, University of Michigan, Ann Arbor, MI 48109

ABSTRACT

This paper presents results of deliberate tailoring of Engineered Cementitious Composites for impact resistance. Microstructure control involving fiber, matrix and fiber/matrix interface was based on steady state dynamic crack growth analyses accounting for rate dependencies of composite phases. Uniaxial tensile stress-strain curves of the resulting impact resistant ECCs were experimentally determined for strain rates ranging from 10^{-5} to 10^{-1} s^{-1}. Drop weight tower test on impact resistant ECC panels and beams were also conducted. Damage characteristics, load and energy absorption capacities, and response to repeated impacts, were studied.

KEYWORDS

ECC, ductile concrete, dynamic fracture, impact resistance, material tailoring

INTRODUCTION

Infrastructure can experience a wide variety of dynamic loads. Severe structural damage or even catastrophic failures have occurred in some extreme events. There is a need to design civil infrastructure resilient to seismic, impact, and blast loading to enhance public safety.

Loading in general, and dynamic loading in particular, can generate tensile stresses in R/C structures. Brittle failure modes including cracking, spalling, and fragmentation of concrete have been observed under impact or blast loading (IBL) [1]. Specifically, studies [2] have shown that the impact resistance of concrete is more closely related to tensile properties than to compressive properties. Although a compressive stress wave is generated on the loading side of the structure by IBL, it reflects as a tensile stress wave after hitting a free boundary on the distal side of the structural element. Fig. 1 shows the numerically simulated stress states [3] at four time instances after a projectile impacted on an object. Tensile stresses (in red) are generated in the impacted material volume at the circumferential edge of the projectile (Fig. 1b and 1c). The compressive stress on the distal side (Fig. 1c) changes into tension when the elastic wave reflects off the traction-free back-face (Fig. 1d).

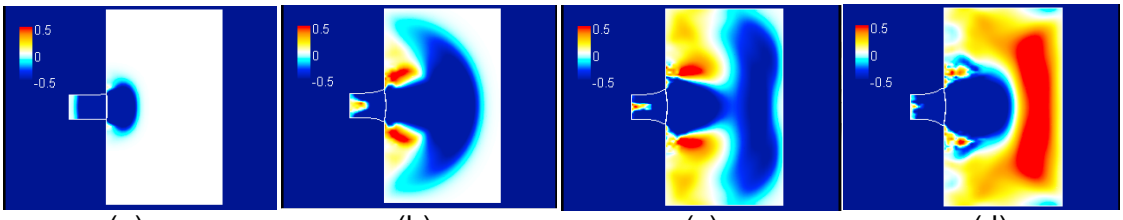

Fig. 1 Numerical simulation of time sequence of stress state in a body under impact (after Shunozuka [3])

The tensile strength of concrete is typically an order of magnitude lower than its compressive strength. In addition, the fracture toughness of concrete, at about 0.01 MPa√m, is among the lowest in construction materials. Therefore, the structural capacity is often limited by the tensile properties of the concrete under IBL. It can be expected that structural integrity loss may be more serious when concrete infrastructure experiences IBL instead of quasi-static loading. Apart from loss of structural integrity, high speed spalling debris ejected from the distal side of the structural elements can cause serious injury to personnel behind the structural elements.

While concrete compressive strength improvements over the last three decades have been impressive, currently attaining over 200 MPa, enhancement of tensile ductility has been achieved only in recent years. Ductile concrete with tensile ductility over 2% has become a reality [4], having been put into full-scale infrastructure such as bridges and buildings [5]. Most studies on ductile concrete have focused on static loading. Investigation of the tensile dynamic response of this class of concrete has just begun. The deliberate engineering of tensile ductility of an Engineered Cementitious Composite (ECC) under high rate loading was recently conducted by Yang [6]. This paper provides a summary of the important findings of this study. What follows is a brief review of the theoretical foundation behind tensile strain-hardening response of ECC under dynamic loading, experimental tensile stress-strain behavior of ECC mixes engineered based on insights gained from the theoretical considerations and micromechanical studies, and comparisons of impact responses of ECC elements versus brittle concrete or mortar.

DYNAMIC ENERGY RELEASE RATE UNDER STEADY STATE CRACK PROPAGATION

The dynamic energy release rate defined as

$$G(\Gamma) = \lim_{\Gamma \to 0} \int_{\Gamma} \left(W + \frac{1}{2}\rho V^2 \frac{\partial u_i}{\partial x}\frac{\partial u_i}{\partial x} \right) dy - \sigma_{ij} n_j \frac{\partial u_i}{\partial x} ds \tag{1}$$

is in general not path independent except for the special case when the crack propagates in a steady state mode [7]. For a steady state crack propagating against a matrix toughness of G_{tip} and crack face bridging traction $\sigma(\delta)$ under remote steady state tensile stress σ_{ss} and steady state crack opening δ_{ss}, it can be shown [6] that

$$G_{tip} = \sigma_{ss}\delta_{ss} - \int_0^{\delta_{ss}} \sigma_B(\delta) d\delta \equiv G_b^{'} \tag{2}$$

using the close contour in Fig. 2.

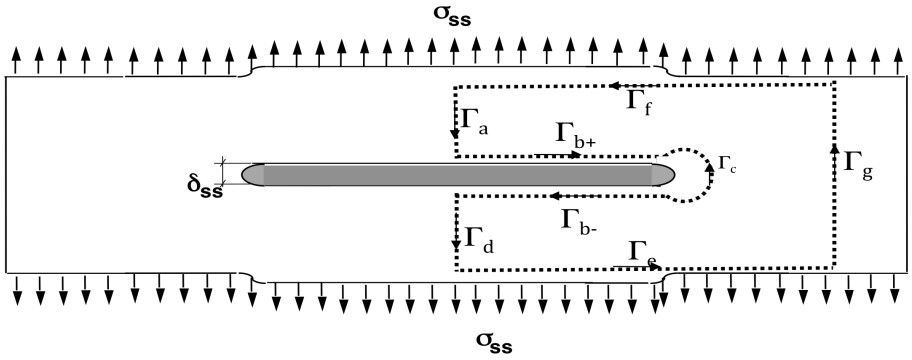

Fig. 2: A contour path for dynamic energy release rate calculation.

This is the same result as for the quasi-static loading case for which V = 0 [8]. This can be expected since the additional kinetic energy term involving V in (1) is a product with $\left(\partial u_i / \partial x\right)dy$. For the horizontal contour dy = 0 while for the vertical contours the $\left(\partial u_i / \partial x\right)$ term is uniformly zero given the steady state crack propagating (in the x-direction) condition. Thus the required balance between matrix toughness G_{tip} and the complimentary energy J_b' is also identical to the quasi-static case. Specifically, since J_b' is limited by its maximum value attained when $\sigma_{ss} = \sigma_o$ when $\delta_{ss} = \delta_o$, the condition for steady state flat crack propagation mode under dynamic or static condition can be stated as

$$G_{tip} < \sigma_o \delta_o - \int_0^{\delta_o} \sigma_B(\delta) d\delta \equiv C \tag{3}$$

where C is the maximum complimentary energy as defined above. In other words, the engineering of fiber reinforced composites for flat crack propagation under dynamic loads follows exactly that under quasi-static loads, with the exception that the matrix toughness G_{tip} and the fiber bridging property $\sigma(\delta)$ may now be loading rate sensitive. Rate sensitivity of $\sigma(\delta)$ may result from the rate sensitivity of the reinforcing fiber or the fiber/matrix interface. This may in turn result in a change in C causing a violation of the inequality sign in (3) at higher loading rate, even when this inequality is satisfied under quasi-static loading condition. In other words, a material that exhibits ductile response under quasi-static loading may respond in a brittle manner under dynamic loading.

Yang and Li [9] studied rate sensitivity of G_{tip} and C, and found that the ratio C/G_{tip} drops by a factor of 2, when the loading speed increases from 0.001 mm/s to 10 mm/s, for a widely studied version of PVA-ECC. Correspondingly, the tensile strain capacity decreases from 3% to 0.5% as the strain rate increases from 10^{-5} s^{-1} to 10^{-1} s^{-1}. The loss of tensile ductility under higher rates of loading is traced to a combined increase in matrix toughness, fiber/matrix interface toughness (a chemical bond), and fiber stiffness, although slightly counteracted by an increase in the strength of the PVA fiber. These micromechanical parameters were experimentally measured.

Eqn. (3) provides insights for the design of ductile ECC resilient to dynamic loading. Specifically, given the sensitivity of fiber/matrix interface toughness to loading rate, hydrophobic fiber may be deliberately chosen to eliminate the fiber/matrix chemical bond, so that only the rate insensitive frictional bond is present. Alternatively, the interfacial transition zone between the fiber and the bulk matrix may be modified to lower the amount of hydration products that chemically binds the fiber to the matrix. One such approach investigated by Yang [6] was to increase the pozzolanic fly ash content in the binder. Fly ash is known to reduce chemical bonding while increasing frictional bonding of the PVA fiber/matrix interface [6] favorable to inducing steady state cracking. In addition, fly ash replacement of cement is also known to lower the matrix toughness. Thus higher fly ash content can be used to compensate the rate sensitivity of the material components that limits the tensile ductility at higher loading rates.

ECC ENGINEERED FOR IMPACT RESISTANCE

Using the micromechanics based model highlighted above, two impact resistant ECC mixes (B and C) were prepared for testing. Their ingredient proportions are shown in Table 1. A control mix A was included. The cement used was Type I Portland Cement from Holcim Cement Co., MI, USA. The water reducing agent used was ADVA Cast 530 from W. R. Grace & Co., IL, USA. Two types of discontinuous polymer fibers, K-II REC™ polyvinyl

alcohol (PVA) fiber from Kuraray Co. Ltd of Osaka, Japan, and Spectra 900 high strength high modulus polyethylene (PE) fiber from Honeywell Inc., USA, were used at 2% volume fraction. The properties of the PVA and PE fibers are shown in Table 2. Pozzolanic admixture used was a low calcium Class F fly ash from Boral, TX, USA. The F110 silica sand with a size distribution from 50 to 250 μm, from US Silica Co., MV, USA, was used.

Mix No.	Cement	Water	Sand	Fly Ash	SP	PE Fiber by volume	PVA Fiber by volume
A	1	0.58	0.8	1.2	0.012	0	0.02
B	1	1	1.4	2.8	0.013	0	0.02
C	1	0.75	0	0	0.013	0.02	0

Table 1 – Mix proportions of Examples, parts by weight

Fiber Type	Nominal Strength (MPa)	Diameter (μm)	Length (mm)	Modulus of Elasticity (GPa)
PVA	1620	39	12	42.8
PE	2400	38	38.1	66

Table 2 – Properties of KII-REC PVA and Spectra 900 PE Fibers

Control mix A represents a PVA-ECC (Mix M45) that has established tensile ductility under quasi-static loading, but experienced a drastic loss under higher rate loading as shown in Fig. 3a. Mix B more than doubles the fly ash content compared to the control mix. The water content is also increased in order to maintain the same water/binder ratio of 0.26. Mix C replaces the hydrophilic fiber by a hydrophobic high modulus polyethylene (PE) Spectra fiber. These measures are meant to reduce the rate dependency of chemical bond and/or impose a larger margin of C/G_{tip}.

Mix No.	Tensile strength (MPa)	Tensile strain capacity (%)	Compressive strength (MPa)
A	8.60	0.90	52.6
B	5.94	3.84	39.6
C	4.19	3.21	48.4

Table 3 – Measured Properties of Example Mixes

Uniaxial tensile test was conducted to characterize the tensile behavior of the composites. The coupon specimen used here measures 304.8 mm x 76.2 mm x 12.7 mm. Tests were conducted in an MTS machine with 25KN capacity under displacement control. The test strain rate ranges from 10^{-5} to 10^{-1} s^{-1}, corresponding to quasi-static loading to low speed impact. Two LVDTs with a gage length of 100 mm measured the deformation during load.

The test results are summarized in Table 3, including tensile strain capacity and strength at the highest test rate (10^{-1} s^{-1}), and compressive strength at quasi-static loading for each mix. Complete tensile stress–strain curves of these composites are shown in Figs. 3b and 3c. Both mixes exhibit significant strain-hardening behavior when subjected to strain rate ranges from 10^{-5} to 10^{-1} s^{-1}. The results show a substantial increase in the ultimate tensile strength with increasing strain rate, while the strain capacity can be retained with similar multiple cracking behavior as those for the static test. Unlike Mix A, the higher strain rates do not seem to negatively affect the strain-hardening behavior of these retailored ECCs.

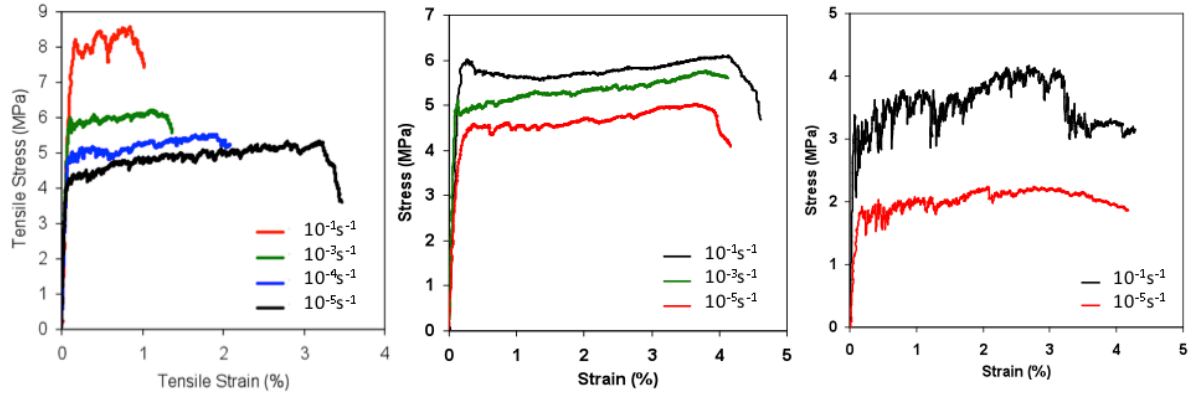

(a) (b) (c)

Fig. 3: Tensile stress-strain curves of (a) ECC M45, (b) HFA-ECC, and (c) PE-ECC, at various strain rates.

IMPACT RESPONSE OF ECC PANELS

Fig. 4 shows an image sequence of the damage process of impact resistant ECC (similar to Mix B) in a drop weight test, using a high-speed camera. The drop mass (flat tup) and drop height were 12 kg and 0.5 m, respectively. The ECC square shaped panel measuring 305mm x 305mm x 25.4 mm (length x height x depth) rested on a steel frame support along its edges. No steel reinforcement was applied to this ECC panel. A puff of dust was observed at impact (Fig. 4a,b) by the loading tup. As the tup rebounded, no damage can be observed on the impact face (Fig. 4c). Examination of the distal side of the panel showed no damage either. Microcracks on this side were observed only after the test was performed three times.

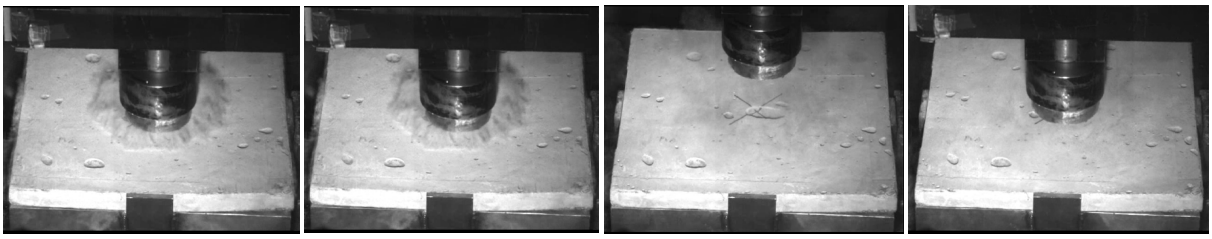

(a) (b) (c) (d)

Fig. 4: High-speed camera image sequence captured at (a) impact, and (b) immediately after impact, (c) tup rebound and (d) tup impacted onto the ECC panel again.

For comparison, the same test was run on a similar size mortar specimen with 0.5% steel reinforcement. In this case, the loading tup penetrated the mortar panel on first impact (Fig. 5). Failure by brittle fracture occurred both around the tup and at one of the corners as the panel bent against the steel support.

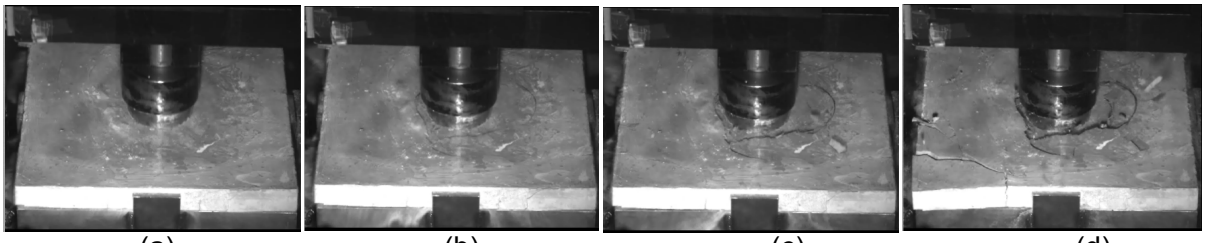

(a) (b) (c) (d)

Fig. 5: High-speed camera image sequence captured (a) at impact, and (b-d) at three time instances immediately after impact.

IMPACT RESPONSE OF ECC AND R/ECC BEAMS

An ECC Mix B beam measuring 305mm x 76mm x 51mm (length x height x depth) and reinforced by a single steel bar was tested under three-point-bending drop weight impacts. The 5mm diameter smooth steel bar was placed close to the bottom side with a clear cover of 18mm. The reinforcing ratio was 0.5%. A control specimen using reinforced concrete (f'_c = 40MPa) was also tested.

A 50kg impact tup with flat impact surface was drop freely from a height of 0.5m onto the specimen center. The mass and height were chosen so that the specimens failed in one single impact. The specimens were supported with a span of 254mm. A steel roller was glued in the middle span and on the top surface of the specimens so that a uniform line load was applied to the specimen when the tup contacted the roller. 1 mm thick hard rubber pads were placed in between the specimen, the roller, and the tup.

Fig. 6 shows the load-deformation curve of the R/C and R/ECC beams. The failure state was defined as when a plateau load capacity (~ 5 kN for both specimens, marked by the two green dots) was reached on softening after peak load. At this stage, pullout of the steel reinforcing bar assumed after a crack completely penetrated through the depth of the specimen. Therefore, the energy capacity of R/C and R/ECC beams was computed as the area below the load-deformation curve until the green dots. While the load capacity of the R/ECC was increased only by 32%, from 22kN to 29kN, the energy capacity was increased by 500% (from 17 N-m to 102 N-m). By comparing with similar tests done on unreinforced beams, Yang [6] attributed the significant energy absorption increase to the high tensile ductility of ECC so that a compatible deformation between steel reinforcement and ECC was achieved during impact, engaging a longer segment of steel to undergo plastic yielding. Synergistic interaction between reinforcing steel and ECC was also observed in other R/ECC elements subjected to quasi-static loading [10].

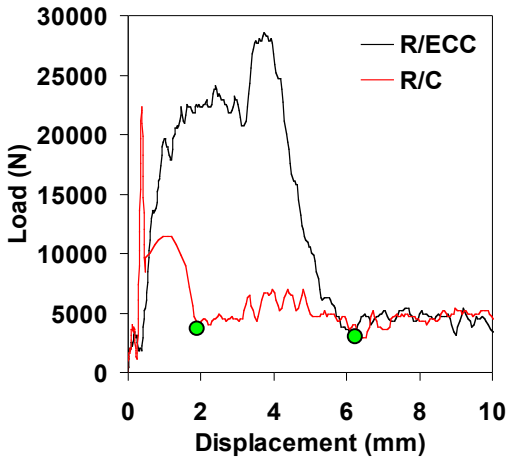

Fig. 6: Load-displacement relationships in single impact experiment.

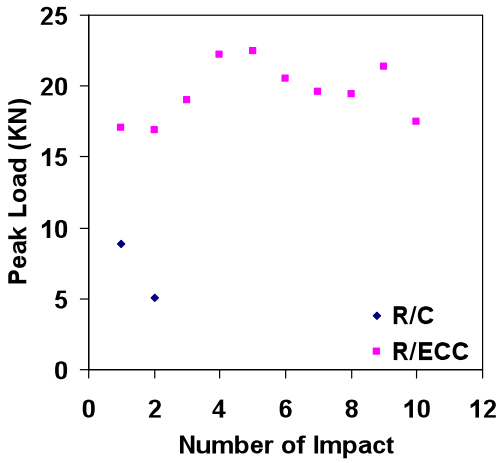

Fig. 7: Peak load recorded in multiple impact experiment.

To evaluate the resistance of R/C and R/ECC beams under multiple impacts, the same test configuration was adopted except that a 12 kg impact tup was chosen and the drop height was reduced to 0.2m. Again, the R/ECC beams showed much improved impact resistance over that of R/C beams. Fig. 7 summarizes the load capacity of R/C and R/ECC beams in each impact. It was found that R/C failed after the first impact at about 9 kN (the data point showing load capacity ~5 kN at the 2nd impact is due to the pullout of reinforcing bar).

However, the load capacity of R/ECC remains roughly constant at about 20 kN over the ten impacts. Fig. 8 shows the damage of R/C and R/ECC after impact testing. As can be seen, one single crack with large crack width appeared in the R/C beam after the first impact. The crack penetrated through the beam causing severe loss of structural integrity and load carrying capacity. In contrast, only very fine microcracks were found in R/ECC specimen even after 10 impacts.

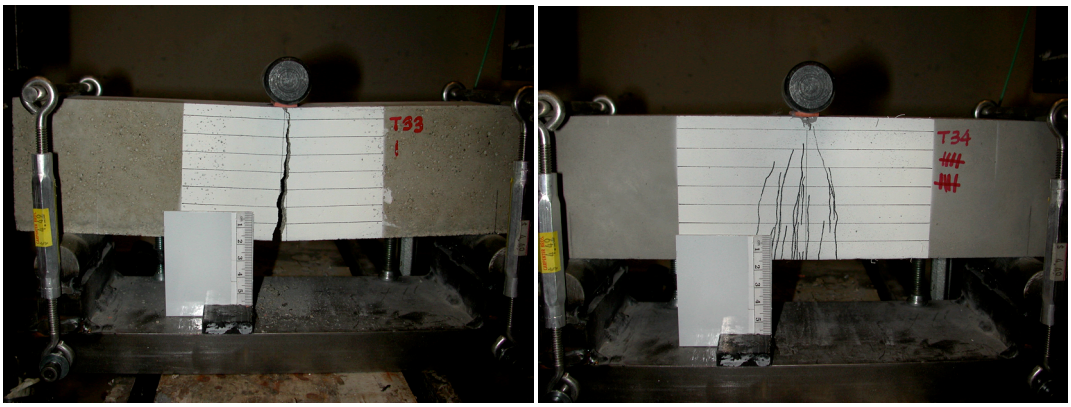

(a) **(b)**

Fig. 8: Damage of (a) R/C beam after the 1st impact (cracking penetrated through specimen) and (b) R/ECC beam after the 10th impact (fine cracks only highlighted by a thick marker).

DISCUSSIONS AND CONCLUSIONS

The improvement of damage tolerance and energy absorption in concrete material is important for enhancing resiliency of civil infrastructure against multi-hazards such as earthquake, projectile and bomb blasts. The impact response of concrete has been widely studied in the last several decades. These studies generally point to the rate sensitivity of concrete that shows a higher strength accompanied by a higher brittleness as the loading rate increases. Previous studies of ECC under increasing loading rate also point to the same phenomena.

In the present study, the intrinsic material source of rate sensitivity in ECC material was identified via dynamic steady state crack propagation analyses. The fracture and microanalyses provide insights into specific selection of fiber, matrix ingredient and interface control to maintain tensile ductility under dynamic loading. By deliberate adjustment of the micromechanical parameters that governs rate sensitivity, it was found that ECC could be tailored to maintain high impact resistance. Specifically, two impact resistant ECC mixes, one containing hydrophobic fiber and the other containing a high dosage of fly ash, demonstrated tensile strain capacity in excess of 3% at all strain rates spanning fours orders of magnitude from 10^{-5} s^{-1} to 10^{-1} s^{-1}. Drop weight tower tests on panels and beams confirmed that the material ductility of impact resistant ECC transformed into enhancements of load and energy absorption capacity of these structural elements. Damage on the impact resistant ECC retained the multiple microcracking characteristics commonly observed in quasi-static loading of regular ECC, thus delaying the localization of a single fracture and allowing the engagement of a longer segment of steel to undergo plastic yielding and energy absorption.

These material and small structural element studies confirm the concept that concrete material can be tailored for resilient infrastructure under impact. However, further studies employing more realistic size specimens, loading type and still higher loading rates are necessary to demonstrate the full effectiveness of ductile ECC for infrastructure protection.

ACKNOWLEGEMENTS

The drop weight impact test on ECC panels was conducted by Dr. Mo Li and Mr. Amit Salvi. Image capture was conducted in the Composite Structures Laboratory directed by Prof. A. Waas.

REFERENCES

[1] Clifton, J.R.:
Penetration Resistance of Concrete – A Review
National Bureau of Standards, Special Publication 480-45, Washington DC (1984)

[2] Malvar, L.J., Ross, C.A.:
Review of Strain Rate Effects for Concrete in Tension
ACI Materials Journal, 95 (1998) No.6, pp.735-739

[3] Shinozuka, J.:
http://www.shinozuka.me.ynu.ac.jp/jshinozu/jshinozu.html#STRESSWAVE, accessed March 29, 2010.

[4] Fischer, G., Li, V.C. (eds):
Proc., International RILEM Workshop on High Performance Fiber Reinforced Cementitious Composites in Structural Applications
Published by RILEM Publications SARL (2006) 580pp.

[5] Rokugo, K., Kanda, T., Yokota H., Sakata, N.:
Applications and recommendations of high performance fiber reinforced cement composites with multiple fine cracking (HPFRCC) in Japan
Materials and Structures (2009) 42:1197–1208

[6] Yang, E.H.:
Designing Functionalities into ECC Materials via Micromechanics
PhD Thesis (2007) Department of Civil and Environmental Engineering, University of Michigan, Ann Arbor, MI (Advisor: Prof. V.C. Li)

[7] Freund, L.B.:
Dynamic Fracture Mechanics,
Cambridge University Press (1990) Cambridge, New York.

[8] Marshall, D.B., Cox, B.N.,
A J-Integral Method for Calculating Steady-State Matrix Cracking Stresses in Composites
Mechanics of Materials, (1988) No.8, pp.127-133

[9] Yang, E.H. and V.C. Li:
Rate Dependence in Engineered Cementitious Composites
Proc., Int'l RILEM Workshop HPFRCC in Structural Applications, published by RILEM SARL (2006) pp. 83-92

[10] Fischer, G., Li, V.C.:
Influence of Matrix Ductility on the Tension-Stiffening Behavior of Steel Reinforced Engineered Cementitious Composites (ECC)
ACI Structural J., 99 (2002) No. 1, pp. 104-111

Corresponding author: Victor C. Li, vcli@umich.edu